

Direct Determination for the  $pK_a$  Values of Radical Cations of NADH Analogues

Shunichi FUKUZUMI\* and Yoshihiro TOKUDA

Department of Applied Chemistry, Faculty of Engineering, Osaka University, Suita, Osaka 565

The  $pK_a$  values of radical cations of NADH analogues, 10-methyl-9,10-dihydroacridine (AcrH<sub>2</sub>) and 9,10-dimethyldihydroacridine (AcrHMe), have been determined directly by measuring the decay of the transient absorption spectra of the radical cations, formed by the electron transfer oxidation with Fe<sup>3+</sup>, through the deprotonation in the presence of various concentrations of perchloric acid in acetonitrile at 298 K.

The biological importance of dihydronicotinamide adenine dinucleotide (NADH) used as an electron source has attracted considerable interest in the electron transfer oxidation of NADH and its analogues, in which the radical cations of NADH and analogues should be formed.<sup>1-3)</sup> We have previously evaluated the  $pK_a$  values of radical cations of NADH analogues by analyzing the kinetic data for electron transfer from NADH analogues to one-electron oxidants such as [Fe(bpy)<sub>3</sub>]<sup>3+</sup> (bpy = 2,2'-bipyridine) in the presence of various bases in MeCN.<sup>4)</sup> On the other hand, Savéant et al. have recently reported the  $pK_a$  value of the radical cation of 10-methyl-9,10-dihydroacridine (AcrH<sub>2</sub>) used as an NADH analogue based on the thermochemical analysis.<sup>5)</sup> The  $pK_a$  value is, however, 8 pH unit lower than the  $pK_a$  value derived from the kinetic analysis.<sup>4,5)</sup> The origin of such large discrepancy for the  $pK_a$  values has remained to be solved, since the  $pK_a$  is one of the most essential properties in understanding mechanisms of the oxidation of NADH analogues. In this study we report the direct determination for the  $pK_a$  values of AcrH<sub>2</sub><sup>•+</sup> and 9-methyl substituted analogue (AcrHMe<sup>•+</sup>) by measuring the decay of the transient absorption spectra of the radical cations through the deprotonation to clarify the origin of the discrepancy for the  $pK_a$  values.

Mixing an acetonitrile (MeCN) solution of Fe(ClO<sub>4</sub>)<sub>3</sub> with AcrH<sub>2</sub> and AcrHMe in a stopped-flow spectrometer results in an instant appearance of a new absorption band at  $\lambda_{max}$  = 640 nm and 660 nm followed by its decay, respectively.<sup>6,7)</sup> Essentially the same transient spectra are obtained when the oxidant Fe(ClO<sub>4</sub>)<sub>3</sub> is replaced by [Fe(phen)<sub>3</sub>]<sup>3+</sup> (phen = 1,10-phenanthroline) or Cu(ClO<sub>4</sub>)<sub>2</sub>. Thus, appearance of a new transient absorption band may be ascribed to formation of radical cation AcrHR<sup>•+</sup> (R = H, Me). In fact, the ESR spectra are observed in the electron transfer oxidation of AcrHR with Fe<sup>3+</sup> in deaerated MeCN by applying a rapid-mixing ESR technique.<sup>7)</sup> A typical example of the decay of AcrHR<sup>•+</sup> (R = Me) is shown in Fig. 1. At the initial stage of the decay obeys the second-order kinetics as shown in the linear plot of [AcrHMe<sup>•+</sup>]<sup>-1</sup> v.s. time. On the other hand, the decay at the longer time obeys the first-order kinetics as shown in the plot of ln(A<sub>0</sub> - A) v.s. time, where A<sub>0</sub> is the initial absorbance at  $\lambda_{max}$  = 660 nm due to AcrHMe<sup>•+</sup> and A is the absorbance at the time t. When the deviation from the second-order plot starts, the first-order decay kinetics begins to hold (Fig. 1). Thus, the decay kinetics of AcrHR<sup>•+</sup> is given by Eq. 1, where  $k_1$  and  $k_2$  are the first-order and the

$$-d[\text{AcrHR}^{\bullet+}]/dt = k_1[\text{AcrHR}^{\bullet+}] + k_2[\text{AcrHR}^{\bullet+}]^2 \quad (1)$$

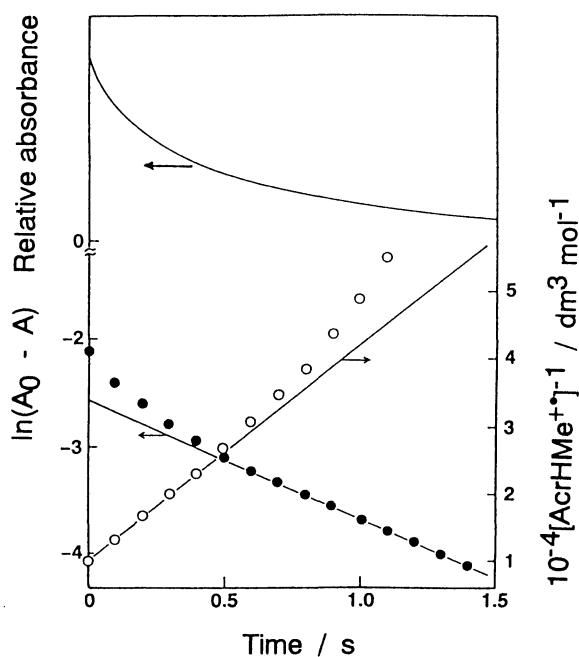


Fig. 1. Decay of the absorbance due to  $\text{AcrHMe}^{+\bullet}$  formed in the electron transfer oxidation of  $\text{AcrHMe}$  ( $1.0 \times 10^{-4} \text{ mol dm}^{-3}$ ) by  $[\text{Fe}(\text{phen})_3](\text{PF}_6)_3$  ( $5.0 \times 10^{-4} \text{ mol dm}^{-3}$ ) in deaerated MeCN at 298 K; the first-order plot (●) and the second-order plot (○).

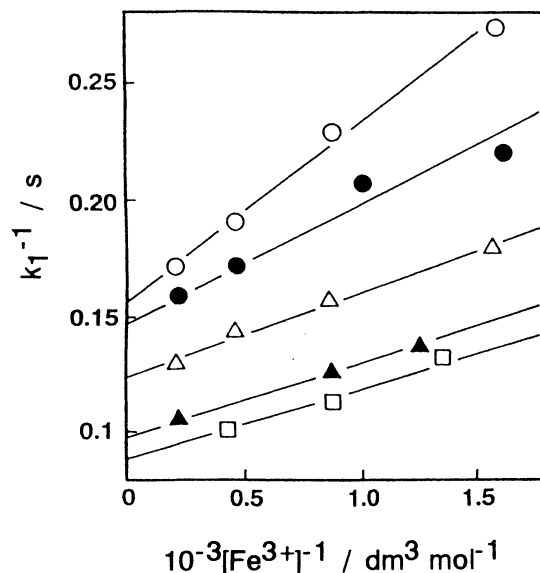


Fig. 2. Plots of  $k_1^{-1}$  vs.  $[\text{Fe}^{3+}]^{-1}$  for the decay of  $\text{AcrH}_2^{+\bullet}$  in the presence of  $\text{HClO}_4$  in deaerated MeCN at 298 K;  $[\text{HClO}_4]$  (70 %) =  $1.2 \times 10^{-2} \text{ mol dm}^{-3}$  (○),  $2.3 \times 10^{-3} \text{ mol dm}^{-3}$  (●),  $5.8 \times 10^{-2} \text{ mol dm}^{-3}$  (Δ),  $8.6 \times 10^{-2} \text{ mol dm}^{-3}$  (▲), and  $1.2 \times 10^{-1} \text{ mol dm}^{-3}$  (□).

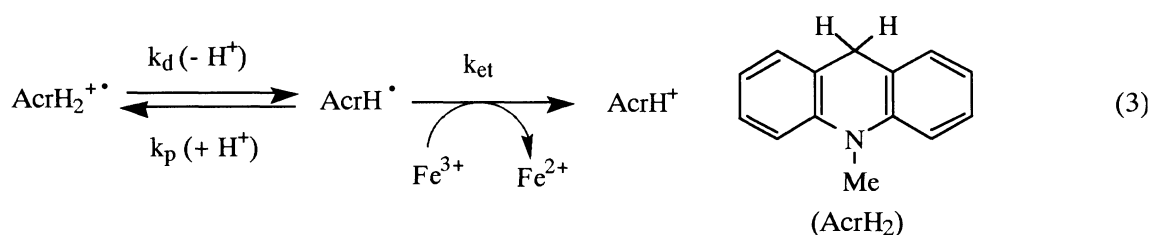
second-order decay rate constants, respectively. The  $k_1$  and  $k_2$  values of  $\text{AcrHR}^{+\bullet}$  are obtained from the slopes of the first-order and second-order plots, respectively. When  $\text{AcrH}_2$  is replaced by the 9,9'-dideuterated compound ( $\text{AcrD}_2$ ), the large primary kinetic isotope effects are observed for both the first-order and second-order decay ( $k_{\text{H}}/k_{\text{D}} = 9.0$  and  $8.0$ , respectively), indicating that both processes involve the transfer of hydrogen nucleus. The second-order decay of  $\text{AcrHR}^{+\bullet}$  may be ascribed to the disproportionation of  $\text{AcrHR}^{+\bullet}$  to yield  $\text{AcrR}^+$  and  $\text{AcrHRH}^+$  (Eq. 2).



The first-order decay ( $k_1$ ) is ascribed to the deprotonation of  $\text{AcrH}_2^{+\bullet}$ , which may be in equilibrium with the protonation of  $\text{AcrH}^{\bullet}$  (Eq. 3). In the oxidation of  $\text{AcrH}_2$  with  $\text{Fe}^{3+}$ , the facile electron transfer from  $\text{AcrH}^{\bullet}$  to  $\text{Fe}^{3+}$  ( $k_{\text{et}}$ ) may also occur to yield  $\text{AcrH}^+$ , judging from the low oxidation potential of  $\text{AcrH}^{\bullet}$  ( $E_{\text{ox}}^0$  vs. = -0.43 V) as compared with that of  $\text{AcrH}_2$  ( $E_{\text{ox}}^0$  vs. SCE = 0.80 V).<sup>4</sup> By applying the steady state approximation to the reactive intermediate radical ( $\text{AcrH}^{\bullet}$ ), the observed first-order decay rate constant  $k_1$  is given by Eq. 4. The plots of  $k_1^{-1}$  vs.  $[\text{Fe}^{3+}]^{-1}$  for the first-order decay of  $\text{AcrH}_2^{+\bullet}$  in the presence of various concentrations of  $\text{HClO}_4$  give straight lines as expected from Eq. 4, as shown in Fig. 2. Similar linear plots are

Table 1. Deprotonation Rate Constants ( $k_d$ ) and  $pK_a$  of  $\text{AcrH}_2^{+\bullet}$  and  $\text{AcrHMe}^{+\bullet}$  in the Presence of  $\text{HClO}_4$  in Deaerated MeCN at 298 K

$[\text{HClO}_4] / \text{mol dm}^{-3}$	$k_d(\text{AcrH}_2^{+\bullet}) / \text{s}^{-1}$	$pK_a(\text{AcrH}_2^{+\bullet})$	$k_d(\text{AcrHMe}^{+\bullet}) / \text{s}^{-1}$	$pK_a(\text{AcrHMe}^{+\bullet})$
$1.2 \times 10^{-2}$	6.4	8.1	$7.0 \times 10^{-1}$	8.5
$2.3 \times 10^{-2}$	6.8	7.6	$8.2 \times 10^{-1}$	8.1
$5.8 \times 10^{-2}$	8.2	7.1	$9.5 \times 10^{-1}$	7.6
$8.6 \times 10^{-2}$	10.3	6.9		
$1.2 \times 10^{-1}$	11.5	6.8		



$$k_1^{-1} = k_d^{-1} + (k_p[\text{H}^+]/k_d k_{et})[\text{Fe}^{3+}]^{-1} \quad (4)$$

obtained for the decay of  $\text{AcrHMe}^{+\bullet}$ . From the intercepts are obtained the deprotonation rate constants  $k_d$ . Since the electron transfer from  $\text{AcrH}^\bullet$  to  $\text{Fe}^{3+}$  may well be assumed to be diffusion-limited, i.e.,  $k_{et} = 2.0 \times 10^{10} \text{ dm}^3 \text{ mol}^{-1} \text{ s}^{-1}$ , the  $pK_a$  [=  $-\log(k_d/k_p)$ ] values are obtained from the intercepts and slopes in Fig. 2. The  $k_d$  and  $pK_a$  values of  $\text{AcrH}_2^{+\bullet}$  and  $\text{AcrHMe}^{+\bullet}$  are summarized in Table 1. The  $k_d$  values increase with an increase in the  $\text{HClO}_4$  concentration, when the  $pK_a$  values decrease. Such changes in the  $k_d$  and  $pK_a$  values may be ascribed to the different concentrations of  $\text{H}_2\text{O}$  contained in the MeCN solution, since  $\text{HClO}_4$  (70 %) was used for a safety reason. In fact, the  $pK_a$  values of  $\text{AcrH}_2^{+\bullet}$  and  $\text{AcrHMe}^{+\bullet}$  decrease with an increase in the  $\text{H}_2\text{O}$  concentration ( $[\text{H}_2\text{O}]/[\text{HClO}_4] = 2.4$ ) contained in the MeCN solution as shown in Fig. 3, where the  $pK_a$  value of  $\text{AcrH}_2^{+\bullet}$  in the presence of added

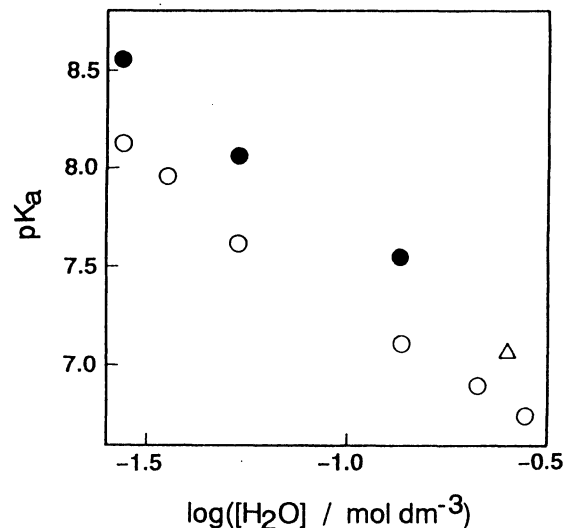


Fig. 3. Dependence of  $pK_a$  of  $\text{AcrH}_2^{+\bullet}$  (  $\circ$  ) and  $\text{AcrHMe}^{+\bullet}$  (  $\bullet$  ) on the  $\text{H}_2\text{O}$  concentration ( $\log[\text{H}_2\text{O}]$ ) in MeCN containing  $\text{HClO}_4$  at 298 K. The ratio of  $[\text{H}_2\text{O}]/[\text{HClO}_4]$ , 2.4 (  $\circ$ ,  $\bullet$  ) and 16.7 (  $\Delta$  ), is changed by addition of  $\text{H}_2\text{O}$  to the reaction system.

H<sub>2</sub>O (0.21 M, [H<sub>2</sub>O]/[HClO<sub>4</sub>] = 16.7) is included. Thus, the deprotonation of AcrH<sub>2</sub><sup>+</sup> is accelerated by the presence of H<sub>2</sub>O, while the protonation of AcrH<sup>•</sup> is retarded, resulting in the significant decrease in the pK<sub>a</sub> values with an increase in the H<sub>2</sub>O concentration in MeCN. Such variation of the protonation and deprotonation rates may be attributed to the strong solvation of H<sub>2</sub>O to H<sup>+</sup> as compared to that of MeCN.<sup>8)</sup>

The Brönsted plot of the deprotonation rate constant *vs.* the pK<sub>a</sub> of bases in H<sub>2</sub>O gave the pK<sub>a</sub> value of AcrH<sub>2</sub><sup>+</sup> as 2.0,<sup>4)</sup> which agrees well with the pK<sub>a</sub> values obtained in this study (pK<sub>a</sub> = 6.8 - 8.1), when the difference in the pK<sub>a</sub> values in MeCN and H<sub>2</sub>O is taken into account (e.g., the pK<sub>a</sub> of pyridine is 12.3 in MeCN, but 5.3 in H<sub>2</sub>O).<sup>5)</sup> The source of the discrepancy concerning the pK<sub>a</sub> values of radical cations of NADH analogues<sup>5)</sup> appears to be the neglect of the significant effects of H<sub>2</sub>O on the pK<sub>a</sub> values in aprotic solvents as clearly demonstrated in Fig. 3.

The present work was supported in part by a Grant-in-Aid for Scientific Research from the Ministry of Education, Science and Culture, Japan.

#### References

- 1) F. H. Westheimer, "Pyridine Nucleotide Coenzymes," ed by D. Dolphin, O. Avramovic, and R. Poulson, Wiley-Interscience, New York (1987), Part A, pp. 253-322; T. C. Bruice, "Progress in Bioorganic Chemistry," ed by F. T. Kaiser, F. J. Kezdy, Wiley, New York (1976), Vol. IV, p. 1; S. Yasui and A. Ohno, *Bioorg. Chem.*, **14**, 70 (1986).
- 2) T. Okamoto, A. Ohno, and S. Oka, *J. Chem. Soc., Chem. Commun.*, **1977**, 181; T. Okamoto, A. Ohno, and S. Oka, *Bull. Chem. Soc. Jpn.*, **53**, 330 (1980); M. F. Powell, J. C. Wu, and T. C. Bruice, *J. Am. Chem. Soc.*, **106**, 3850 (1984); B. W. Carlson, L. L. Miller, P. Neta, and J. Grodkowski, *ibid.*, **106**, 7233 (1984); S. Fukuzumi, Y. Kondo, and T. Tanaka, *J. Chem. Soc., Perkin Trans. 2*, **1984**, 673; S. Fukuzumi, S. Mochizuki, and T. Tanaka, *J. Am. Chem. Soc.*, **111**, 1497 (1989); S. Fukuzumi, S. Mochizuki, and T. Tanaka, *Inorg. Chem.*, **29**, 653 (1990); A. Ohno, M. Ogawa, Y. Mikata, and M. Goto, *Bull. Chem. Soc. Jpn.*, **63**, 813 (1990).
- 3) S. Fukuzumi and T. Tanaka, "Photoinduced Electron Transfer," ed by M. A. Fox and M. Chanon, Elsevier, Amsterdam (1988), Part C, pp. 578-636; S. Fukuzumi, "Advances in Electron Transfer Chemistry," ed by P. S. Mariano, JAI press, Greenwich (1992), Vol. 2, pp. 67-175.
- 4) S. Fukuzumi, S. Koumitsu, K. Hironaka, and T. Tanaka, *J. Am. Chem. Soc.*, **109**, 305 (1987).
- 5) P. Hapiot, J. Moiroux, and J.-M. Savéant, *J. Am. Chem. Soc.*, **112**, 1337 (1990); A. Anne, P. Hapiot, J. Moiroux, P. Neta, and J.-M. Savéant, *J. Am. Chem. Soc.*, **114**, 4694 (1992).
- 6) S. Fukuzumi, S. Mochizuki, and T. Tanaka, *J. Chem. Soc., Dalton Trans.*, **1990**, 695; A. Anne, P. Hapiot, J. Moiroux, P. Neta, and J.-M. Savéant, *J. Phys. Chem.*, **95**, 2370 (1991).
- 7) S. Fukuzumi and T. Kitano, *Chem. Lett.*, **1990**, 1275.
- 8) D. T. Sawyer and J. S. Valentine, *Acc. Chem. Res.*, **14**, 393 (1981).

(Received May 18, 1992)